

# Statistical Fourier Descriptors for Defect Image Classification

Fabian Timm and Thomas Martinetz  
*Institute for Neuro- and Bioinformatics, University of Lübeck,  
 Ratzeburger Allee 160, 23538 Lübeck, Germany*

## Abstract

*In many industrial applications, Fourier descriptors are commonly used when the description of the object shape is an important characteristic of the image. However, these descriptors are limited to single objects. We propose a general Fourier-based approach, called statistical Fourier descriptor (SFD), which computes shape statistics in grey level images. The SFD is computationally efficient and can be used for defect image classification. In a first example, we deployed the SFD to the inspection of welding seams with promising results.*

## 1. Introduction

Machine vision systems are widely used in process industry to optimise the quality of the production process. However, the major difficulty is that of finding appropriate features, especially when the specification of the problem is imprecise. The time needed for classifying a new sample can usually be neglected, whereas feature extraction has to be computationally efficient and powerful.

Since shape is one of the most important low-level image features, feature extraction approaches that describe the shape of an object are often used in industrial applications as well as in computer vision applications. One of the best known shape descriptors is the Fourier descriptor [2]. Although this approach is over 30 years old, it is still found to be a valid shape description tool. In several comparisons, the Fourier descriptor has proved to outperform most other boundary-based methods in terms of accuracy and efficiency [4, 7, 11]. However, Fourier descriptors cannot be applied to images with overlaying objects or to grey level images.

In this paper, we propose a new Fourier-based feature extraction approach for grey level images called *statistical Fourier descriptor* (SFD). This descriptor covers the “statistics of shapes” for a given grey level

image by decomposing the image into a stack of binary images. We apply this descriptor to the problem of welding seam inspection and compare results to other feature extraction methods that can describe textures and shapes.

## 2. Fourier-based Object Description

It is common to all Fourier-based shape descriptors that the boundary line of a two-dimensional object is presented using some one-dimensional function  $f(k)$ , i.e. the shape signature. One of the simplest ways to obtain a shape signature is to combine the coordinates  $(x_k, y_k)$  of the boundary points  $k = 0, \dots, N - 1$  to a complex number, i.e.  $f(k) = x_k + j y_k$ . However, this shape signature has to be periodic in order to be used for the 1D discrete Fourier transform. In general, there are three different methods for obtaining a periodic shape signature: equal points sampling, equal angle sampling and equal arc-length sampling. Among these methods, the equal arc-length sampling achieves the best equal space effect and therefore a unit speed of motion along the shape boundary [9]. Obviously, the number of sampling points  $N$  determines the accuracy of the approximation. Using only a small number of sampling points yields two advantages at the same time: the shape is smoothed and the Fourier transform is computed efficiently.

### 2.1. Fourier Descriptors

Since the shape signature is represented by a one-dimensional periodic signal, it can be transformed to the frequency domain using the discrete Fourier transform (DFT). The DFT of a shape signature  $f(k)$  consisting of  $N$  samples is then given by

$$F_n = \sum_{k=0}^{N-1} f(k) e^{-j2\pi nk/N}, \quad 0 \leq n \leq N - 1 \quad (1)$$

where  $F_n$  are the transform coefficients of  $f(k)$  and known as Fourier descriptors. The Fourier descriptors

are often expressed in polar form  $F_n^* = |F_n| e^{j\phi_n}$ . By transforming to the frequency domain several geometric transformations of the shape can be related to simple operations. For example, translation of the shape only affects the first Fourier coefficient or scaling the shape with a factor of  $a$  leads to a scaling of the Fourier coefficients by  $a$ . Furthermore, the coefficients can be normalised to be invariant towards the starting point by subtracting the phase of the second Fourier descriptor, weighted by  $n$ , from the phase of all Fourier descriptors:

$$F_n^* \leftarrow F_n^* e^{-j\phi_1 n} . \quad (2)$$

Then, the starting point is approximately at angle 0. A detailed explanation of the properties of Fourier descriptors can be found in [3].

A common approach to shape analysis is to use only a subset of low-frequency coefficients. This covers most of the shape information and removes high frequency noise.

## 2.2. Statistical Fourier Descriptors

Since the Fourier descriptor approach can only be used in binary images, we propose a new Fourier-based method, called *statistical Fourier descriptor* (SFD), that describes shape statistics in grey level images. We use the following decomposition scheme [10, 8] (see Fig. 1): For a given input image we generate a stack of  $M$  binary images (A) and compute the connected (white and black) components (B). For each component  $c$  we compute a feature vector  $\mathbf{g}_c^b$  for black components and a feature vector  $\mathbf{g}_c^w$  for white components that contains the magnitude and the phase of the corresponding  $N$  Fourier descriptors (C):

$$\mathbf{g}_c^* = (|F_0|, \dots, |F_{N-1}|, \phi_0, \dots, \phi_{N-1})^T . \quad (3)$$

Then, for the  $i$ th binary image the local shape features of  $N_c$  components are combined such that (D):

$$\bar{\mathbf{g}}_i^* = (\boldsymbol{\mu}, \boldsymbol{\sigma}, \mathbf{m}, \theta, \rho)^T \in \mathbb{R}^{3 \cdot 2N+2} , \quad (4)$$

$$\mu_i = \frac{1}{N_c} \sum_{c=0}^{N_c-1} g_{cl}^* , \quad (5)$$

$$\sigma_i = \sqrt{\frac{1}{N_c} \sum_{c=0}^{N_c-1} (g_{cl}^* - \mu_i)^2} , \quad (6)$$

$$m_i = \max_c \{g_{cl}^*\} , \quad (7)$$

$$\mathbf{d} = \frac{1}{N_c} \sum_{c=0}^{N_c-1} (\mathbf{c}_c - \mathbf{c}_I) , \quad (8)$$

where  $\theta$  and  $\rho$  are the orientation and magnitude of the displacement vector  $\mathbf{d}$ ,  $\mathbf{c}_c$  is the centre of component

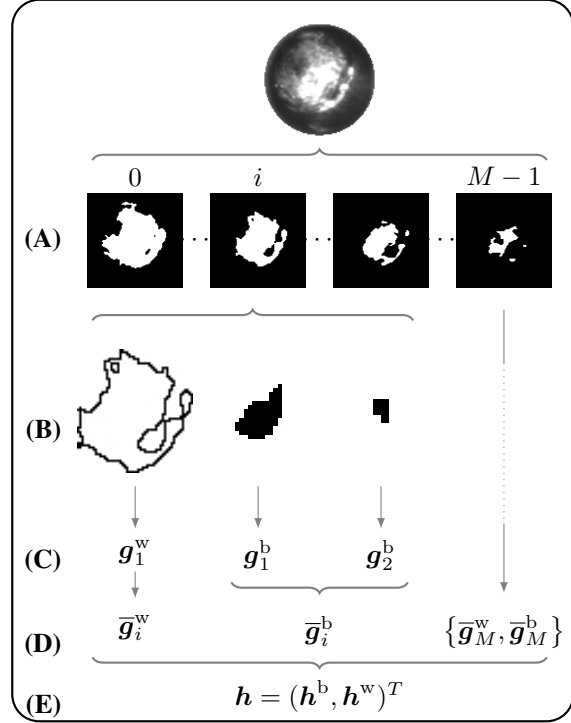


**Figure 1. Decomposition scheme for a given input image. See text for explanations.**

$i$ , and  $\mathbf{c}_I$  is the image centre. Using the properties of the displacement vector, we can distinguish between binary images where the components are located circularly around the centre and binary images where the components are located at one particular side of the image.

In the last step, we combine the local features of the  $M$  binary images by calculating statistics, i.e. mean, standard deviation, maximum, and sample mean, to obtain a single feature vector  $\mathbf{h} = (\mathbf{h}^b, \mathbf{h}^w)^T \in \mathbb{R}^{48N+16}$  for a given input image (E):

$$\mathbf{h}^* = (\boldsymbol{\gamma}, \boldsymbol{\delta}, \boldsymbol{\varepsilon}, \boldsymbol{\eta})^T \in \mathbb{R}^{4 \cdot (6N+2)} , \quad (9)$$

$$\boldsymbol{\gamma}_i = \frac{1}{M} \sum_{i=0}^{M-1} \bar{\mathbf{g}}_{il}^* , \quad (10)$$

$$\boldsymbol{\delta}_i = \sqrt{\frac{1}{M} \sum_{i=0}^{M-1} (\bar{\mathbf{g}}_{il}^* - \boldsymbol{\gamma}_i)^2} , \quad (11)$$

$$\boldsymbol{\varepsilon}_i = \max_i \{\bar{\mathbf{g}}_{il}^*\} , \quad (12)$$

$$\boldsymbol{\eta}_i = \left( \sum_{i=0}^{M-1} \bar{\mathbf{g}}_{il}^* \right)^{-1} \sum_{i=0}^{M-1} i \bar{\mathbf{g}}_{il}^* . \quad (13)$$

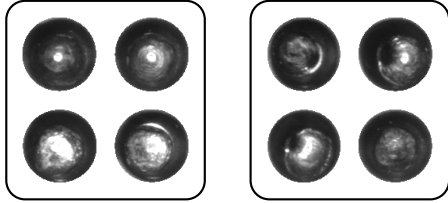


**Figure 2. Example images of defect-free (left) and defective weldings (right).**

Let  $N$  be the number of sampled points on the boundary, then for a given input image, the SFD computes a feature vector with  $48N + 16$ . For large  $N$  this feature vector becomes very high-dimensional and thus the performance of certain classifiers might be poor. Therefore, a method for selecting relevant features is suggested.

### 3. Defect Image Classification

We apply the SFD approach to the optical inspection of welding seams. The dataset contains 657 images of defect-free weldings and 277 images of defective weldings. Each image was labelled by experts, scaled to different number of grey levels (16, 32, 64, 128, 256) and smoothed by a Gaussian filter to reduce noise. Example images of both classes are shown in Fig. 2. The large variance of different defects cannot be described easily and a feature extraction method that covers specific image properties such as the shape and position of objects at different grey levels is required. Hence, the SFD is an appropriate method for feature extraction in this case.

For the SFD, we use the equal arc-length sampling on the boundary with 64 points and compute the phase and the magnitude of the Fourier coefficients as local shape features. Since the positions, the rotation, or the size of the components might be relevant properties, we don't normalise the Fourier coefficients concerning to this. We only scale the coefficients to be invariant towards the starting point of the shape signature (see Eq. 2). We further compare the performance of the SFD to other feature extraction methods, i.e. Statistical Geometric Features (SGF) [10] and Specularity Features (SPEC) [8].

#### 3.1. Feature Selection and Classification

Finding a method that selects a subset of features yielding the best performance in terms of classification accuracy is ongoing research. Since a SFD feature vector can be of very high dimension and the SFD features

can also be significantly correlated, we select relevant features while minimising redundancy by a common correlation analysis. First, we sort the features by their correlation coefficient with the labels. Second, starting with the feature that obtains the largest correlation coefficient, we add a succeeding feature if its maximum correlation with the existing features is smaller than a user-set threshold  $\tau$ . We proceed until we have selected  $L$  features. Using this very simple method, we obtain a feature set where each feature itself has a high discriminance and a low redundancy. For our experiments we set  $\tau = 0.2$  and  $L = 200$ , but the results are insensitive towards slight changes of these values.

The support vector machine (SVM) [1] has become a very powerful approach for classification. Standard two-class SVMs require samples that describe both classes properly. In our case, however, there are only a few defective samples that are characterised well. Therefore, we apply a one-class SVM [5] in order to increase the robustness against unknown classes of outliers. We choose a Gaussian kernel and evaluate the best parameters by 10-fold cross validation. For a comparison of the different feature extraction methods we apply a Wilcoxon signed rank test to the test errors.

#### 3.2. Results and Discussion

Classification results for the different feature extraction methods are shown in Fig. 3. First, performance of the SFD and SGF is increased rapidly by using a larger number of grey levels (from over 17% error down to 11%). This indicates that components of binary images at several grey levels are relevant for these welding images. By taking less than 128 grey levels too many components with different shapes will be merged together.

Second, the best performance of the SFD with an error of 11.3% is achieved by using images with 256 grey levels (8 bit), although there is no significant difference compared to images with 128 grey levels (7 bit). The SGF yield their best performance with an error rate of 12.5% using 128 grey levels. The superior performance of the SFD compared to SGF is very significant ( $p = 0.05$ ).

Third, the SPEC features slightly outperform the SFD and SGF with an error rate of 9.5% at 64 grey levels. However, this slight outperformance is significant ( $p = 0.03$ ,  $p = 0.01$ ). Further, the change in performance for different numbers of grey levels is not as significant as for the other two approaches.

Since the SPEC features were explicitly designed for the inspection of welding seams, they achieve the best overall performance. However, for some applications it is quite hard to determine appropriate local shape fea-

tures. By employing the Fourier descriptor, we cover almost all shape properties of an object and are able to combine them to shape statistics. If we further apply a feature analysis method, we can identify relevant shape statistics and reduce the amount of features.

The statistical Fourier descriptor may also be used for other applications such as surface inspection of LED chips [6] or texture classification. In cell nuclei classification, for example, the texture of the nucleus has to be classified (see Fig. 4). If we decompose the image into its binary images, we can see clearly that some of the objects in these binary images change while others stay almost constant. We need to verify the performance of the SFD also for these images, but so far the results are quite promising. However, there are no benchmark datasets available for the problem of defect image classification. Most of the related publications, especially from the field of wafer inspection, don't make their images available. Therefore, it is very hard to make any comparison to existing approaches which are, indeed, mostly developed for a particular dataset.

Although the SFDs were only applied to grey level images, they can easily be extended to colour images.

#### 4. Conclusions

We have proposed a new Fourier-based approach for feature extraction, called statistical Fourier descriptor (SFD). The SFD is a general approach for feature extraction and covers shape statistics of grey level images. It is computationally efficient and can easily be extended to colour images.

In a first experiment, we have applied the SFD to the inspection of welding seams. Although the SFD performs slightly worse than the features that were explicitly designed for this application, the results are promising. Especially for applications where it is not really clear which shape features are relevant, the SFD is an appropriate tool for feature extraction.

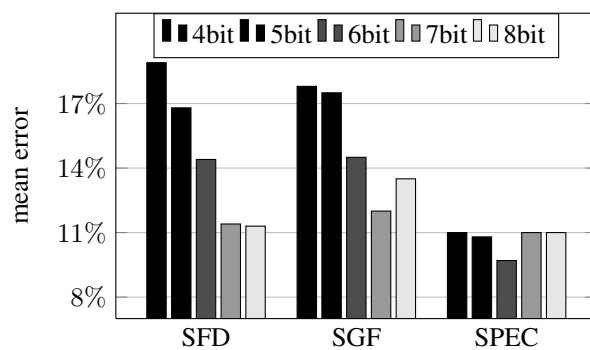


Figure 3. Performance comparison.

#### References

- [1] C. Cortes and V. Vapnik. Support-vector networks. *Machine Learning*, 20(3):273–297, 1995.
- [2] G. H. Granlund. Fourier preprocessing for hand print character recognition. *IEEE Trans. Computer*, 21(2):195–201, 1972.
- [3] A. K. Jain. *Fundamentals of Digital Image Processing*. Prentice Hall Information and Systems Science Series, Upper Saddle River, NJ, USA, 1989.
- [4] H. Kauppinen, T. Seppanen, and M. Pietikainen. An experimental comparison of autoregressive and Fourier-based descriptors in 2D shape classification. *IEEE TPAMI*, 17(2):201–207, 1995.
- [5] K. Labusch, F. Timm, and T. Martinetz. Simple incremental one-class support vector classification. In *Proc. of the 30th DAGM*, Lecture Notes in Computer Science, pages 21–30. Springer, 2008.
- [6] H.-D. Lin and C.-Y. Chung. A wavelet-based neural network applied to surface defect detection of LED chips. In *Proc. of the 4th ISNN*, Lecture Notes in Computer Science, pages 785–792. Springer, 2007.
- [7] B. M. Mehtre, M. S. Kankanhalli, and W. F. Lee. Shape measures for content based image retrieval: A comparison. *Inf. Process. Manage*, 33(3):319–337, 1997.
- [8] F. Timm, S. Klement, T. Martinetz, and E. Barth. Welding inspection using novel specular features and a one-class SVM. In *Proc. of the Int. Conference on Imaging Theory and Applications*, pages 146–153. INSTICC, 2009.
- [9] P. J. van Otterloo. *A Contour-oriented Approach to Shape Analysis*. Prentice Hall International (UK) Ltd., Hertfordshire, UK, 1991.
- [10] R. Walker and P. T. Jackway. Statistical geometric features: Extensions for cytological texture analysis. In *Proc. of the 13th ICPR*, pages 790–794. IEEE Computer Society Press, 1996.
- [11] D. S. Zhang and G. J. Lu. A comparative study of curvature scale space and Fourier descriptors for shape-based image retrieval. *Journal of Visual Communication and Image Representation*, 14(1):39–57, 2002.

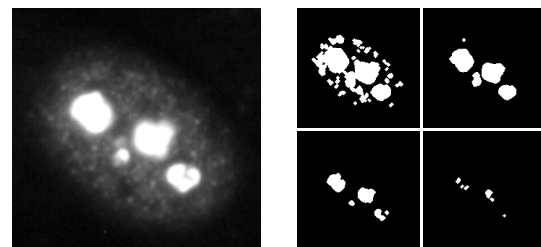


Figure 4. Image of a cell nucleus (left) and the stack of binary images (right).